Radial frequency patterns describe a small and perceptually distinct subset of all possible planar shapes

Gunnar Schmidtmann[a], Ingo Fruend[b,*,1]

[a] Eye & Vision Research Group, School of Health Professions, University of Plymouth, Plymouth, Devon, UK
[b] Centre for Vision Research, and Department of Psychology, York University, Toronto, ON, Canada

A B S T R A C T

The visual system is exposed to a vast number of shapes and objects. Yet, human object recognition is effortless, fast and largely independent of naturally occurring transformations such as position and scale. The precise mechanisms of shape encoding are still largely unknown. Radial frequency (RF) patterns are a special class of closed contours defined by modulation of a circle's radius. These patterns have been frequently and successfully used as stimuli in vision science to investigate aspects of shape processing. Given their mathematical properties, RF patterns can not represent any arbitrary shape, but the ability to generate more complex, biologically relevant, shapes depicting the outlines of objects such as fruits or human heads raises the possibility that RF patterns span a representative subset of possible shapes. However, this assumption has not been tested before. Here we show that only a small fraction of all possible shapes can be represented by RF patterns and that this small fraction is perceptually distinct from the general class of all possible shapes. Specifically, we derive a general measure for the distance of a given shape's outline from the set of RF patterns, allowing us to scan large numbers of object outlines automatically. We find that only between 1% and 6% of naturally smooth outlines can be exactly represented by RF patterns. We present results from a visual search experiment, which revealed that searching an RF pattern among non-radial frequency patterns is efficient, whereas searching an RF pattern among other RF patterns is inefficient (and vice versa). These results suggest that RF patterns represent only a restricted subset of possible planar shapes and that results obtained with this special class of stimuli can not simply be expected to generalise to any arbitrary planar shape.

1. Introduction

The visual system is exposed to a vast number of natural and artificial objects and shapes. Regardless, human object recognition is effortless and fast (Biederman, 1987; Thorpe, Fize, & Marlot, 1996), and is largely insensitive to naturally occurring variations in position, size, perspective, and illumination (Gauthier & Tarr, 2016; Pinto, Cox, & DiCarlo, 2008; reviewed by DiCarlo, Zoccolan, & Rust, 2012). Although the surface properties of objects (e.g. texture, colour etc.) are important for object recognition, it is their outlines that have traditionally been the focus of object recognition models (Biederman, 1987; Marr & Nishihara, 1978). Yet while the visual system presumably contains efficient mechanisms for encoding outline shapes, both natural and artificial, structural properties of these mechanisms remain largely unknown.

Since their introduction by Wilkinson, Wilson, and Habak (1998),

Radial Frequency (RF) patterns have been frequently used to investigate aspects of shape processing. The relatively simple mathematical definition of RF patterns and the ease with which they can be generated and modulated has made RF patterns a popular stimulus in psychophysical (reviewed by Loffler, 2008; Loffler, 2015), physiological, and imaging studies (Salmela, Henriksson, & Vanni, 2016; Wilkinson et al., 2000).

Several psychophysical and modeling studies have suggested that different RF patterns are processed by different mechanisms (Bell & Badcock, 2009; Bell, Badcock, Wilson, & Wilkinson, 2007, 2009; Jeffrey, Wang, & Birch, 2002; Loffler, Wilson, & Wilkinson, 2003; Poirier & Wilson, 2006; Schmidtmann, Kennedy, Orbach, & Loffler, 2012). Some of these studies have reported evidence that the visual system contains narrowly-tuned RF channels (Bell & Badcock, 2009; Bell et al., 2007; Bell, Wilkinson, Wilson, Loffler, & Badcock, 2009). Two subsequent studies by Dickinson and colleagues have, however,

---

rejected the idea of RF shape channels. Dickinson, Bell, and Badcock (2013) suggested that the relevant cue that distinguishes the patterns with different radial frequencies is the angle subtended between adjacent points of maximum curvature at the pattern centre. More recently, and in line with these findings, Dickinson, Haley, Bowden, and Badcock (2018) showed that RF patterns and similar patterns with rectified sinusoidal modulations but the same overall triangular-like shape, were very hard to discriminate, which resulted in steep functions describing response time versus set size in a visual search task. In summary, these results argue against the existence of discrete RF shape channels. Yet, the ability to generate biologically relevant stimuli depicting the outlines of objects such as fruits or human heads (Wilson, Wilkinson, Lin, & Castillo, 2000; Wilson & Wilkinson, 2002; Wilson, Loffler, & Wilkinson, 2002), might suggest that the visual system utilizes RF patterns to encode object parts. However, any form of this argument requires that superpositions of RF components (so called RF compounds) can in some way generalize to arbitrary stimuli. Wilkinson et al. (1998) already noted mathematical limitations in RF patterns (and compounds) and pointed out their significant differences from, for example Fourier shape descriptors, which can in principle be used to create any kind of closed two-dimensional shape (Alter & Schwartz, 1988; Zahn & Roskies, 1972). Despite this limitation, there remains the possibility that RF compounds span a representative subset of possible shapes. However, this assumption has not been tested before. Here we provide theoretical and experimental evidence that RF compounds represent a restricted subset of possible planar shapes and we show that this special class of stimuli is perceptually different from arbitrary planar shapes. Thus, results with RF patterns and compounds can not simply be expected to generalize to arbitrary planar shapes.

2. Material and methods

2.1. Subjects

Seven subjects participated in this study (4 females, 29.4 ± 6.7 years mean $\pm$ STD). Subjects had normal or corrected-to-normal visual acuity and were naive as to the purpose of the experiment. Informed consent was obtained from each subject. The experiments were approved by the University of Plymouth Ethics Committee and were conducted in accordance with the original Declaration of Helsinki.

2.2. Apparatus

The experiments described below were performed using *PsychoPy* (Peirce, 2007). The stimuli were presented on a LG Studioworks 700S CRT monitor (17″) with a resolution of 800×600 pixel and a refresh rate of 85 Hz (mean luminance: $65 \frac{cd}{m^2}$) under the control of a 3.3 GHz Mac mini. The observers viewed the stimuli at a distance of 40 cm, which was maintained by a chin and forehead rest. At this viewing distance one pixel subtended 0.055deg visual angle.

2.3. Stimuli

We analyzed a set of 391 animal outlines from the Hemera Photo database. These outlines have been used before (Fruend & Elder, 2013). The photographs contain blue screened animals and we extracted their outlines as high resolution polygons by using Moore neighbourhood tracing on the images' alpha channel. Each polygon was then downsampled to a 120 corner equilateral polygon and represented by its sequence of turning angles. Note that turning angles provide a discrete approximation to the shape's curvature.

We created a sample of 391 closed, non-intersecting random outlines that matched the marginal turning angle distribution of the 391 animal outlines. We used population Monte Carlo (Cappé, Guilin,

Marin, & Robert, 2004), starting with 391 circles. At each step of the algorithm, each of the 391 outlines was randomly perturbed using the technique developed by (Fruend & Elder, 2013, see also Elder, Oleskiw, & Fruend, 2018) and the resulting, perturbed outlines were re-sampled based on the fit with the target distribution. This procedure leads to a fair sample from the maximum entropy distribution of closed, non-intersecting shapes that match the marginal turning angle distribution of the animal outlines. Specifically, these shapes are from a larger set of possible shapes than the animal outlines and provide a better approximation to the notion of "general shapes with naturalistic smoothness."[2]

The diameter of the shapes ranged from $\varnothing_{min} = 0.67$deg to $\varnothing_{max} = 1.43$deg of visual angle (see Fig. 5).

2.4. Procedure

The stimuli used in this study were either approximate RF compounds (30 shapes with lowest RF error, see Eq. (5)), or non-RF patterns (30 shapes with highest RF error). Thus, a total of 60 shapes from the set of 391 random shapes were used in the experiment. We conducted a visual search experiment with four conditions which were tested in separate experimental blocks. The target shapes could be an RF compound or non-RF pattern and were paired in the following way:

- RF compound target vs. RF compound distractors
- RF compound target vs. non-RF distractors
- non-RF target vs. RF compound distractors
- non-RF target vs. non-RF distractors

We employed a single-target visual search task (Treisman & Souther, 1985; see Wolfe & Horowitz, 2004; Wolfe & Horowitz, 2017 for reviews). An experimental trial was initiated by setting the monitor to a mid grey background. The observer started an experimental block by pressing a key on a computer keyboard. A central circular white fixation dot ($\varnothing = 0.14$deg) was presented throughout the entire experiment. During the first interval, the observer was presented with a target-shape (RF compound or non-RF) presented at the centre of the screen (see Fig. 1), followed by the presentation of the search display and mask display. The shapes in the search display were located at 5deg eccentricity from the centre of the screen and were equally distributed on a circle around the central fixation dot. For example, in the case where the search display contained 2 shapes, these were presented at opposing sides, whereas for the search display containing 4 shapes, these would form a square (like in Fig. 1). The exact angular position of the shapes was randomly determined. The search display could contain the target shape at a random position or only distractor shapes, either RF compound or non-RF shapes (see conditions above). The search display was immediately followed by a mask display (see Fig. 1). The stimulus presentation time for each search display was controlled by a QUEST adaptive procedure (Watson & Pelli, 1983), using implementations from *PsychoPy* (Peirce, 2007). The task of the observer was to decide whether the search display contained the target shape or not, by pressing one of two keys on a computer keyboard. Each condition was tested 3 times during an experimental session, leading to 12 blocks per session. The target stimuli were selected at random. Observers received feedback on incorrect decisions. These were indicated by a red fixation dot ($\varnothing = 0.57$deg). The experiment was repeated for 2, 4, and 8 shapes in the search display.

To ensure that the presentation time manipulation was maximally effective and to avoid additional cues from potential afterimages or transient signals, a mask was presented immediately after the stimulus display. The mask consisted of all distractor outlines of the respective search display. For target trials, an additional outline from the

---

[2] Note that non-smooth outlines neither look very natural, nor can they be described as RF compounds.
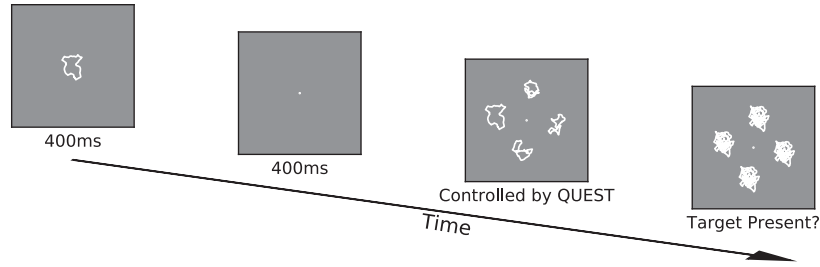
Fig. 1. Trial structure in the search experiment. On every trial, the observer first saw a target shape for 400 ms, followed by a 400 ms fixation interval. After the fixation interval, $n \in \{2, 4, 8\}$ shapes were presented for a duration controlled by an adaptive staircase procedure. When the presentation interval was over, the shapes were immediately followed by a mask that consisted of n superimposed shapes from the set of distractors (all distractor shapes from the current trial plus one additional random shape on target trials). The mask remained visible until the observer pressed a button to indicate if they saw a target or not.

respective distractor class was selected at random and added to the mask. These outline stimuli were randomly rotated and superimposed to construct the mask for a single location. These single location masks were then presented at the same locations as the target and distractor outlines of the respective trial.

2.5. Feature analysis

We analyzed how well different shape features correlated with the extent to which a shape could be represented as a compound RF pattern. By construction all artificial shapes used here had the same outline length. We analyzed the area of the shapes, given by

$$A = \frac{1}{2} \left| \sum_{n=1}^{N} x_n y_{n+1} - y_n x_{n+1} \right|,$$

where the shape is given as a polygon with corner points (x_n, y_n), $n = 1, ..., N$ and $x_{N+1} = x_0, y_{N+1} = y_0$. Furthermore, we analyzed the mean unsigned curvature approximated by the average absolute value of the polygon's turning angles. The power spectrum of natural outlines is typically well approximated by a power law, such that the slope of the spectrum in double logarithmic coordinates gives an indication for how strong the low pass characteristic of the power spectrum is. Specifically, let $c_n = x_n + iy_n$ and $C_f, f = -N/2...N/2$ denote the Fourier coefficients of c_n. We used linear regression to get the slope b from the relationship

$$2\log_{10}|C_f| = a + b\log_{10}|f|.$$

Finally, we analyzed two properties of the shape's skeleton representation, namely the number of branching points and the average length of skeleton branches. For that, we derived the skeleton from the Voronoi transformation of the shape's outline points (Mayya & Rajan, 1996).

3. Results

3.1. Quantifying distance from the set of compound radial frequency shapes

In general, an RF compound is a circle with radius given as[3]

$$R(t) = 1 + \sum_{j=1}^{M} A_j \sin\left(\omega_j t - \theta_j\right). \tag{1}$$

---

[3] Note that other authors use θ instead of t here and ϕ_i instead of θ_i. We decided to use the Latin character t here, because that is more common for a continuous variable that parameterizes a shape. We decided to also use θ as the offset, partly because it makes the relationship to t more clear and partly because we were using ϕ for the function that maps t to general rotation angles.

The outline of an RF compound is then given as the set $\widetilde{S}_{RF}$ of all points x and y, such that there exists a t with

$$x = R(t)\cos(t), \quad y = R(t)\sin(t). \tag{2}$$

Here, we are only interested in whether or not a given shape can be represented as an RF compound, but we are not interested in how many components M are needed to do so. Thus, if there is a function $R(t)$, such that Eq. (2) holds, we can use a one dimensional Fourier transform to get to the representation (1). We would like to emphasize that this really pushes the RF representation to its limit and goes beyond the kinds of compound RF patterns typically used in the literature.

A key point of the following exposition is that a shape can only be represented as an RF compound if and only if it can be drawn in a continuous rotation around a centre point. To simplify some of the notation, we will describe shapes as sets parameterized by a closed, simple curve in the plane of complex numbers. A general form of an RF compound is then

$$S_{RF} = \{z \in \mathbb{C} : z = c + R(t)\exp(it) \text{ for one } t \in \mathbb{R}\}, \tag{3}$$

with a continuous function R, where $R(t) > 0$, $i = \sqrt{-1}$ and an appropriately chosen center $c \in \mathbb{C}$. In order to obtain a closed curve, we further require that R is periodic with period 2π, such that $R(t) = R(t + 2\pi)$. Note that the function R is typically specified as a superposition of sine and cosine components as in Eq. (1). By requiring that R is periodic with period 2π, a Fourier series expansion of R exists and consists of this superposition of sine and cosine components.

Although it is known that not all possible planar shapes can be represented as RF compounds (see Fig. 2C for an example), we would like to have a criterion if a given shape S can be expressed as an RF compound. For this, we first note that we can write any *arbitrary* shape in polar coordinates relative to a center $c \in \mathbb{C}$ to yield

$$S = \{z \in \mathbb{C} : z = c + r(t)\exp(i\phi(t)) \text{ for one } t \in \mathbb{R}\}, \tag{4}$$

with both r and ϕ being continuous functions with period 2π. Fig. 2 shows examples of shapes with their corresponding radius functions $r(t)$ and rotation functions $\phi(t)$.

Note the similarity between Eq. (4) and Eq. (3). If ϕ is invertible, we can re-parameterise t by $\widetilde{t} = \phi^{-1}(t)$ and arrive at

$$S = \{z \in \mathbb{C} : z = c + r(\widetilde{t})\exp(i\phi(\widetilde{t})) \text{ for one } t \in \mathbb{R}\}$$
$$= \{z \in \mathbb{C} : z = c + r(\phi^{-1}(t))\exp(it) \text{ for one } t \in \mathbb{R}\}.$$

Thus, if ϕ is invertible, S is an RF compound with $R(t) = r(\phi^{-1}(t))$. For closed and continuous outlines, ϕ is always continuous (modulo 2π) and surjective. Thus, ϕ is invertible if and only if ϕ is monotonic (modulo 2π, see Fig. 2). Note, that the center c determines the form of r and ϕ and it may be possible that an invertible ϕ exists relative to one choice of the center point but not relative to another choice of the center point.
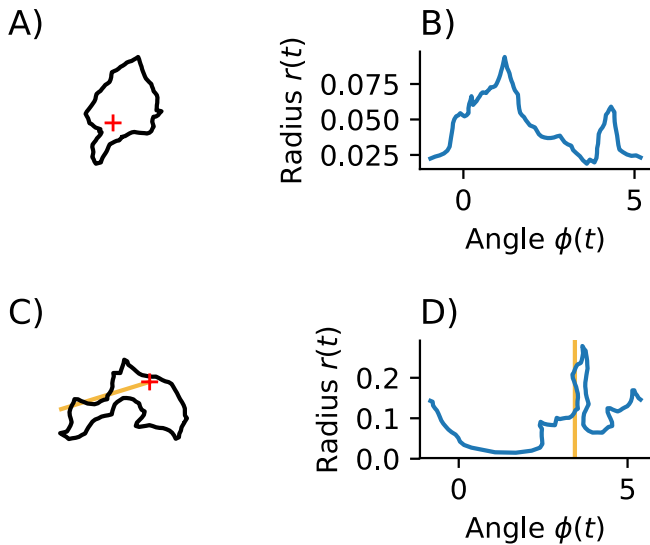
Fig. 2. Examples of radius and rotation functions for two example shapes. **A** An example shape that can be represented as an RF compound. The center of the RF compound is marked by a red cross. **B** Radius vs. rotation angle curve for the outline shape in part A. Although both r and ϕ are functions of t, r could in this case equally be interpreted as a function of ϕ. **C** An example shape that cannot be represented as an RF compound. A possible center location is marked by the cross. **D** Radius vs. rotation angle curve for the outline shape in part C. Because $\phi(t)$ is not monotonous, r cannot be interpreted as a function of ϕ without reference to t. In particular, note that for the $\phi = 3.44$ marked by the orange line, there are multiple different radii. For reference, the rotation angle $\phi = 3.44$ is marked as an orange ray in part C as well.

In practice, a shape will be given as a polygon with corners p_n, $n = 1, ..., N$. We can express these points in polar coordinates relative to a center c as $p_n = r(p_n, c)\exp(i\phi(p_n, c))$.[4] In order to determine if a given polygon can be represented as an RF compound, we search the interior of the polygon for a centre point that minimizes the error function

$$E(c) = \frac{1}{N} \sum_{n=1}^{N} (\phi(p_n, c) - \phi(p_{g(n)}, c))^2, \tag{5}$$

where g sorts the polar angles of the points such that $\phi(p_{g(0)}, c) \leqslant \phi(p_{g(1)}, c) \leqslant \cdots \leqslant \phi(p_{g(N)}, c)$. If we can find a c such that $E(c) = 0$, the shape is an RF compound. To determine c in practice, we performed a grid search over 35×35 points that spanned the entire interior of the analyzed polygon. Code to replicate this analysis can be found at https://github.com/fruendlab/rf-checker/releases/tag/paper-version.

3.2. Compound radial frequency patterns span a small subset of all possible shapes

Fig. 3A shows an example outline that can be represented as an RF compound. The red cross marks the center of the pattern. Note that being representable as an RF compound depends on the choice of this center point. The shading of colour inside the outline in Fig. 3A indicates how well the outline can be represented as an RF compound, with darker colours indicating a less faithful representation as an RF compound according to Eq. (5).

As outlined in Section 3.1, an outline can be represented as an RF compound if and only if the shape can be drawn in a continuous rotation around the centre point (marked as a cross in Fig. 3A). In Fig. 3B,

---

[4] Note that r and ϕ take different arguments than in the previous paragraph. However, they correspond to discrete versions of the same functions. To emphasize this point, we decided to use the same notation here.
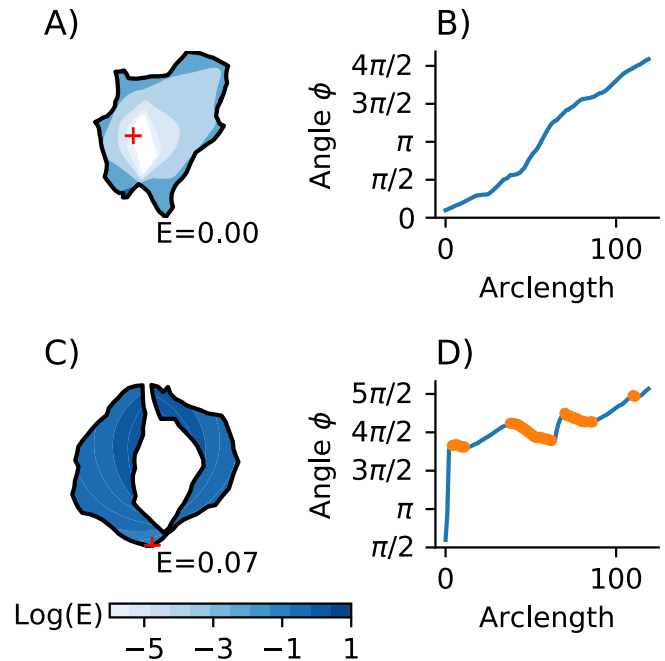

Fig. 3. Not all stimuli can be faithfully represented as RF compounds **A** Stimulus that can be faithfully represented as a compound RF pattern. Colors code the log-error (see Eq. (5)) incurred when choosing the respective location as center. The $+$ marks a location at which the error is minimized and takes a value of 0 in this case. **B** Angle function associated with the outline in part A. **C** Stimulus that cannot be faithfully represented as a compound RF pattern. Representation like in part A. **D** Angle function associated with the outline in part C. Locations that violate the monotonicity are marked in orange.

we show the rotation angle function associated with the outline in Fig. 3A. Indeed, the function is monotonically increasing. However, this does not have to be the case for every planar outline. We show a counter example in Fig. 3C; this shape cannot be approximated as an RF compound. Fig. 3D shows the rotation angle function around the best point of this outline (marked by a cross in Fig. 3C). As expected, this function is not increasing monotonically.

Are outlines like the one in Fig. 3C the exception or the rule? We used the criterion derived in Eq. (5) to analyze 391 random smooth polygons with a distribution of turning angles that matched the distribution of turning angles found in natural object outlines. These outlines potentially span a larger set than the set of all possible object outlines, while they are still naturalistic in the sense that they are piecewise smooth. We find that only 4 of these outlines are exact RF compounds in the sense that the monotonicity error of the rotation angle function is below machine precision (see Fig. 4A). In other words, only 1.02% of outlines from this set corresponds to a compound RF pattern. Furthermore, for only a few outlines did the deviations from a compound RF structure remain minor. Fig. 4B-G illustrates this point; even the outline that corresponds to the 20-th percentile of the distribution (Fig. 4C) has features that can not be represented by a compound RF pattern (for example the little tip at the lower left). Thus, only a small fraction of outlines can be represented as RF compounds.

One might argue that these artificial shapes are particularly difficult to describe using compound RF patterns. We therefore also analysed a set of 391 animal outlines from the Hemera database. These animal outlines are a real subset of all possible natural planar shapes. Thus, we expect the results found on these outlines to provide an approximate upper bound on the fraction of shapes that can be faithfully represented as compound RF patterns. For the animal shapes, 23 outlines (5.88%) could be faithfully represented as RF compounds. However, the remaining distribution was essentially the same as for the artificial shapes (see orange line in Fig. 4A).
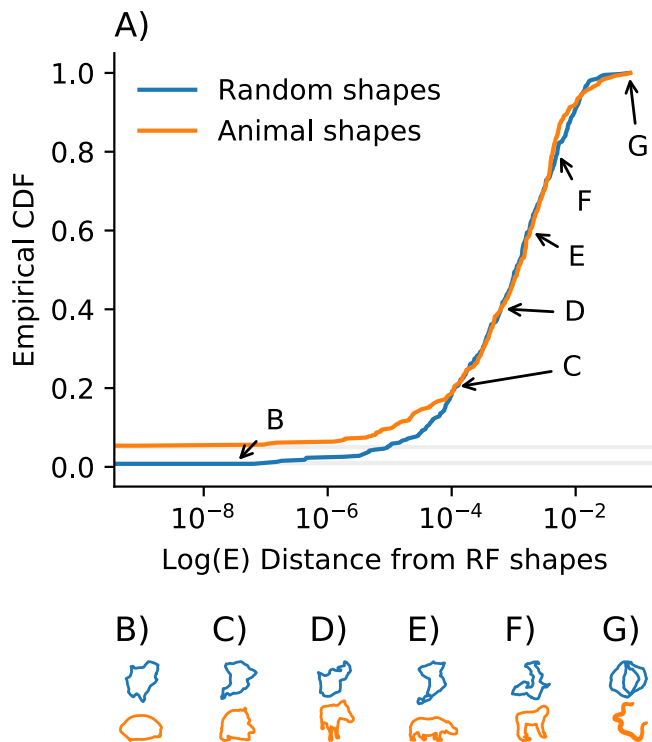
Fig. 4. Distribution of distances from the set of RF compounds. **A** Empirical cumulative distribution (CDF) function of the distance to the set of compound RF patterns. Note that the x-axis is logarithmically scaled. The horizontal gray lines mark the lower 1% and the lower 5% of the distribution. The locations marked by the arrows correspond to approximately the 0, 20, 40, 60, 80, and 100-th percentile and examples corresponding to these locations are shown in panels **B–G**. The orange distribution function was obtained on a selection of 391 animal outlines from the Hemera database.

Fig. 5. All stimuli used in the search experiment. **A** Stimuli that can be well represented as compound RF patterns. **B** Stimuli that can be particularly badly represented as compound RF patterns. Note that the outlines for some of the examples from B have some extremely narrow parts, where the outline appears to touch or intersect itself. However, we verified that this was not the case for any of these shapes.

Looking at Fig. 4A, we note that although the lower tail of the distribution of distances from the set of RF compounds differs between these fairly different classes of shapes, the distributions are almost the same above the 20th percentile (marked by C). Thus, although the number of outlines that can be *exactly* represented as an RF compound pattern might to some extent differ between different classes of shapes, there are in both cases at least 80% of the shapes that can definitely not be represented as RF compound patterns.

3.3. The subset of shapes that is spanned by compound radial frequency patterns is perceptually distinct

It might be that—although being quantitatively rare—compound RF patterns are representative examples of the set of all possible shape outlines. If this was the case, it should be equally easy to search for an RF compound within a set of compound RF distractors as it is to search for an RF compound within distractors that cannot be represented as RF compounds. To test this hypothesis, we used the visual search task described in Section 2.4. We chose the 30 stimuli with the smallest distance from the set of compound RF patterns as "RF-like" patterns and the 30 stimuli with the largest distance from the set of compound RF patterns as outlines that were clearly not RF compounds (see Fig. 5). On every trial observers (N = 7) first saw an example outline and then had to indicate if that outline was contained in a set of outlines presented briefly afterwards (see Fig. 6A for an example display), followed by a mask. During the experiment, we varied the presentation time of the search display to determine the time required for 75% correct performance.

If observers were searching for a compound RF target within an search display of RF compounds (blue line in Fig. 6B), the required presentation

time increased from 335.2 $\pm$ 62.0 ms (mean $\pm$ s.e.m) for two shapes to 881.8 $\pm$ 41.9 ms for eight shapes. Similarly, threshold presentation time increased from 367.1 $\pm$ 43.9 ms for two shapes to 995.4 $\pm$ 103.6 ms for eight shapes if observers were searching for a non-RF pattern in a non-RF patterns search display. However, threshold presentation times were much shorter (138.1 $\pm$ 30.5–243.3 $\pm$ 16.7 ms for a non-RF target with compound RF distractors and 74.8 $\pm$ 23.9–139.1 $\pm$ 31.7 ms for compound RF target with non-RF-distractors) and did not significantly increase with the number of outlines in the search display (Pearson correlation between number of outlines and presentation time $r = 0.16$, $p = 0.33$), if observers had to search for an RF compound in non-RF distractors and vice versa.

In order to analyze these results statistically, we performed a repeated measures ANOVA with factors "number of locations" and "condition". This analysis revealed significant main effects for the number of locations ($F(1, 5) = 20.08$, $p < 0.01$) and of condition ($F(3, 15) = 85.31$, $p < 10^{-8}$). More importantly, there was a significant interaction between these two factors ($F(3, 15) = 12.13$, $p < 0.001$), reflecting the fact that not only did the average presentation time depend on the condition, but also the slope of the search function.

3.4. Representability as a compound RF pattern correlates with many known shape features

To understand how our shape representability index from Eq. (5) is related to other shape features, that are known to be relevant for shape perception, we analyzed the correlation between $E(c)$ and the area of the shapes, the average absolute curvature, the slope of the power spectrum of the shape's outline, the number of branches of their Voronoi skeleton, and the average length of branches of the Voronoi skeleton.

Fig. 7A shows Spearman's rank correlations between $E(c)$ and each of the analyzed shape features for the 391 random shapes. Although, by construction, each of the random shapes had the same outline length, there were clear differences in the shapes' area that correlated strongly with the representability index from Eq. (5) (Spearman's $\rho = -0.838$, $p < 10^{-10}$ based on Ramsey's, 1989's Edgeworth approximation). We also found that the number of branches of the Voronoi skeleton strongly correlated to the shape's representability as an RF compound, with more branches correlating with less faithful representation ($\rho = -0.435$, $p < 10^{-10}$). Furthermore, we found that the slope of the power spectrum of the shape's outline correlated with the representability as a RF compound ($\rho = -0.226$, $p < 10^{-5}$). Thus, shapes with a less low-pass power spectrum tended to be likely representable as a compound RF pattern. Other features, such as the average unsigned
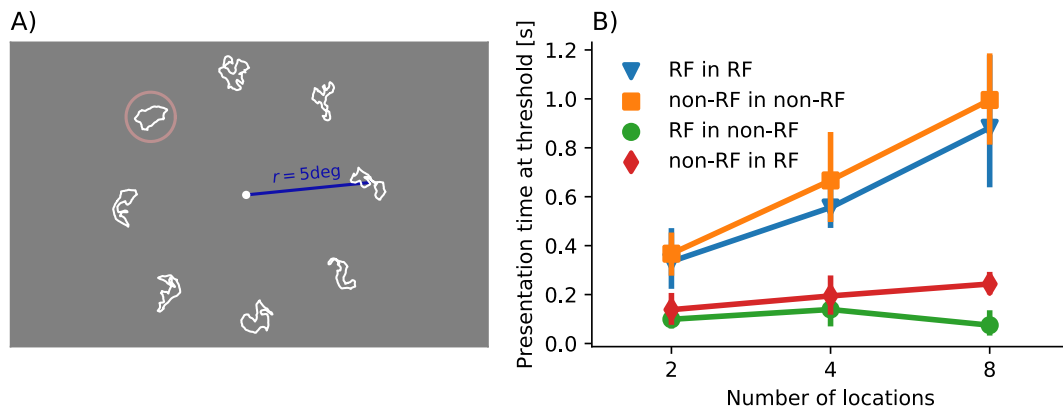
Fig. 6. Search is efficient if target and distractors differ in how well they can be represented as an compound RF pattern. **A** Example of a search display with 8 search locations. Here, an RF compound (pink circle, not shown in the actual experiment) is the target, while the distractors are all non-RF patterns. Shapes were shown as white outlines (width = 0.055deg) on a gray background and at an excentricity of 5 degree visual angle. **B** Average presentation time required to achieve 75% correct performance. Error bars indicate 95% confidence intervals based on bootstrap sampling. If target and distractor differ in how well they can be represented as an RF compound, search was efficient and did not change much with the number of possible target locations. If target and distractor were both compound RF patterns or both non-RF patterns, search was inefficient and threshold presentation time increased with the number of possible target locations.

curvature of the outline, or the average length of skeleton branches did not significantly correlate with the representability index (average signed curvature $\rho = -0.098$, $p = 0.0545$, average length of skeleton branches $\rho = 0.004$, $p > 0.9$).

Fig. 7B shows a similar analysis restricted to the shapes that were used in the search experiment. Specifically, we asked if there was a significant difference in one shape feature between the compound RF and the non-RF shapes used in the experiment and Fig. 7B shows t-values associated with this comparison. This analysis largely confirmed the previous results obtained on the full set of random shapes, with the exception that there was also a significant difference in the average length of branches of the Voronoi skeleton ($t = -2.185$, $p < 0.05$). Taken together, these results suggest that being representable as an RF compound is not necessarily a perceptual quality of shape in itself, but it rather correlates with many perceptually relevant qualities of shape.

4. Discussion

RF patterns have been widely and successfully applied as visual stimuli in many domains of vision science, ranging from visual psychophysics to brain imaging, and clinical research, which have lead to many important insights in shape processing (reviewed by Loffler, 2008, 2015). It is important to emphasize that in showing the limitations of compound RF patterns, it is not our intention to invalidate the application of (compound) RF patterns as visual stimuli in vision science. In fact, it is clear that RF patterns (and compounds) allow targeted experimental manipulations for a number of behaviourally relevant shape classes, as shown by their application in the representation of fruits and outlines of synthetic faces (Wilson et al., 2000; Wilson & Wilkinson, 2002; Wilson et al., 2002).

Instead, it was our aim to test whether compound RF patterns can generalize to *any* arbitrary planar shape. To do so, we provide a novel and fast method to determine the distance of a given shape's outline from the set of RF compounds. The results from this analysis show that only a small subset, approximately 1–6% (see Fig. 4), of all smooth outlines can be exactly represented as RF compounds. This new algorithm will allow the vision science community to find an optimal RF compound patterns that can be used to represent any arbitrary planar shape (i.e. optimal within the limitations of RF compounds). The code can be found at https://github.com/fruendlab/rf-checker/releases/tag/paper-version.

To understand if compound RF patterns are also perceptually an exception, we have employed a single-target visual search task (Wolfe &

Horowitz, 2004, 2017). The rationale for this visual search approach was that if RF compounds are a representative class of the set of all possible planar shapes, the performance to search a compound RF pattern within a set of compound RF distractors should be similar to the performance to search for a compound RF pattern within non-RF shapes. Our results clearly show that this is not the case. Results show that searching an RF compound among non-RF patterns is efficient, whereas searching an RF compound among other RF compounds is inefficient (and vice versa, see Fig. 6).

Note that previous visual search studies have typically presented a target stimulus embedded in distractor shapes of the same type (Treisman & Souther, 1985; see Wolfe & Horowitz, 2004, 2017 for reviews). In the experiments described here, the distractors in the search display were all different, either compound RF or non-RF shapes. The aim of the experiment described was to capture an entire class or distribution of shapes, i.e. RF compounds or non-RF shapes. Hence, each search display contained different, randomly selected distractor shapes. The disadvantage of this method is, however, that it does not allow us to determine which of the distractor shapes lead to incorrect decisions.

Also note that the compound RF patterns used in this study are different compared to previous studies. Specifically, we used simple white lines with a width of 0.055deg, whereas most previous studies employed RF stimuli and compounds with a cross-sectional luminance profile typically defined by a fourth derivative of a Gaussian or Gaussian profile. More importantly, the method used here generates a combination of many RF patterns, whereas most previous studies used either *single component* RF patterns (e.g. Bell & Badcock, 2008, 2009; Bell et al., 2007; Green, Dickinson, & Badcock, 2017, 2018a, Green, Dickinson, & Badcock, 2018b; Hess, Achtman, & Wang, 2001; Jeffrey et al., 2002; Schmidtmann et al., 2012; Loffler et al., 2003), combinations of two (Bell & Badcock, 2009; Bell et al., 2007; Lawrence et al., 2016) or three RF components (Schmidtmann, Jennings, & Kingdom, 2015). Given that the aim of this study was to explore the limits of what can be represented by compound RF patterns, the stimuli used here are combinations of an arbitrary number of RF patterns (see Methods). It should however be noted, that this involves a number of very high radial frequency components that would be unlikely to contribute to a really useful shape representation and that cannot be reliably discriminated by human observers (Wilkinson et al., 1998).

It is important to mention that some previous visual search studies have employed planar shapes. Most notably, Kristjánsson and Tse (2001) measured search performance for a variety of ellipses and semiellipses, where the latter contained curvature discontinuities. Their
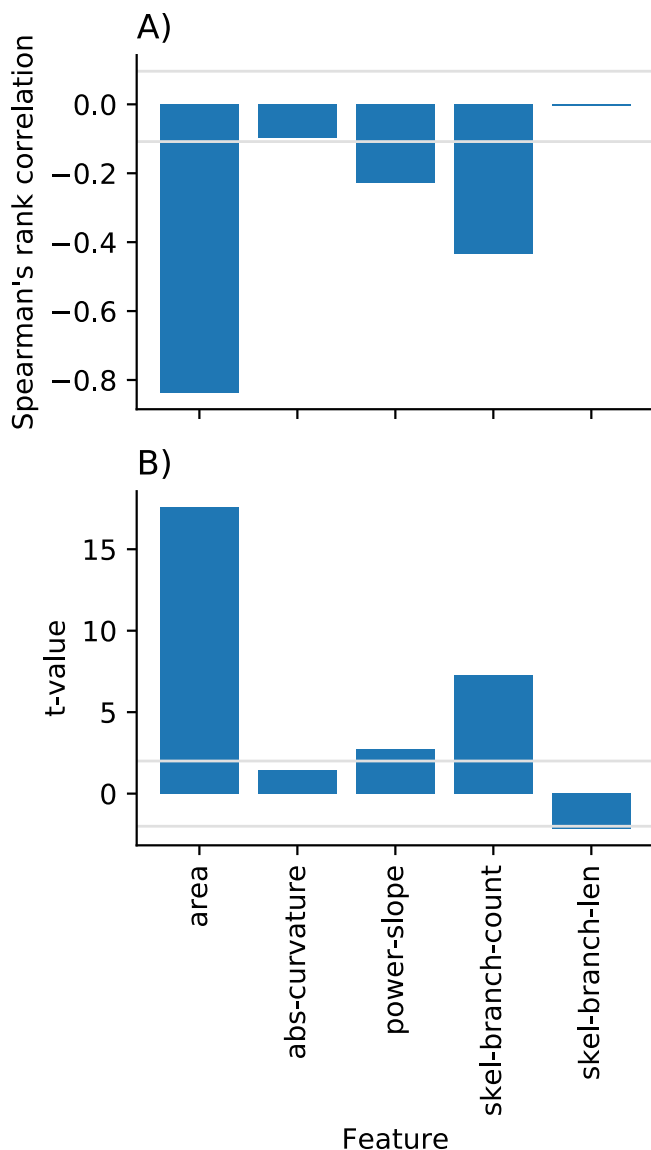
Fig. 7. Well known shape features correlate with representability as a compound RF pattern. **A** Spearman's rank correlation between a shape's representability index from Eq. (5) and different shape features across 391 random shapes. Shape features were *area*: the area of the interior of the shape, *abs-curvature*: average absolute curvature as a measure of overall edgyness, *power-slope*: slope of the power spectrum of the shape's outline, *skel-branch-count*: number of branches of the Voronoi skeleton, *skel-branch-len*: average length of skeleton branches. Light gray lines denote critical values ($\alpha = 5\%$) based on the method by Ramsey (1989). **B** t-values for comparison between rf and non-rf shapes used in the experiment. Light gray lines indicate critical values ($\alpha = 5\%$ two-sides) for an unpaired t-test.

results showed that embedding a semiellipse in ellipse distractors elicited efficient search, which led them to conclude that the curvature discontinuities in these semiellipses act as cues. However, Dickinson et al. (2018) recently revisited these results and measured search performance for Kristjánsson and Tse's stimuli as well as for a range of RF patterns and showed that the efficient search is not mediated by curvature discontinuities, but rather shape cues, specifically adjacent points of maximum curvature. In another recent visual search study, (Ehinger & Wolfe, 2016) iteratively optimized distractor shapes to make search of a (compound) RF representable target either efficient or

inefficient. In that study, they used compound RF patterns as in our Eq. (1) to achieve an efficient parameterization of a large shape space and they found that searching for an RF compound target in RF compound distractors can be either efficient or inefficient depending on how the distractors were constructed. However, it should be noted that these authors explicitly used their observers' behaviour to guide an optimization algorithm to find target-distractor combinations for which visual search for an RF compound target in RF compound distractors is efficient. It seems that this is a special case and that without explicit optimization of the target-distractor combinations, search for RF compounds within RF compounds is more typically inefficient. Looking at Fig. 5, this does not seem very surprising. This is also corroborated by the observation in Section 3.4 that weather or not a shape can be represented as an RF compound pattern correlates with many established perceptually meaningful shape features. We believe that the work by Ehinger and Wolfe (2016) nicely illustrates the usefulness of RF compounds for vision research. However, these authors' data did not address the perceptual differences between shapes that can be represented as compound RF patterns and those that can not.

Our conclusions depend to some extent on the assumption that curvature-matched random shapes are an appropriate way to capture the full variability of naturally occurring planar shapes. As already pointed out in Section 3.2, we believe that it is likely that these random shapes tend to overestimate the variability of naturally occurring planar shapes. On the other hand, we believe that the population of animal shapes analyzed in Section 3.2 tends to underestimate this variability. Above the 20th percentile, the distributions of our compound RF representability index are almost the same for these two classes of shapes. Thus, the true number of shapes that can be represented as RF compound patterns is likely going to be somewhere between the $\approx 1\%$ found for the random shapes and the $\approx 6\%$ found for the animal shapes and definitely not larger than 20%. In addition, it has been found that the curvature-matched random shapes provide a relatively good approximation to the perceptual qualities of true natural shapes (Fruend & Elder, 2013): Humans can not tell apart outline fragments up to about a quarter of the full shape from fragments of natural shapes. This suggests that these random shapes are a suitable first order approximation to the set of all naturally occurring shape outlines.

The results presented in this paper raise the question whether there are alternative, more universal shape descriptors? In a relevant study, Fruend and Elder (2015) attempted to evaluate the efficiency of a variety of alternative shape descriptors, namely, Fourier Descriptors (Alter & Schwartz, 1988; Zahn & Roskies, 1972), Shapelets (Dubinskiy & Zhu, 2003) and Formlets (Elder, Oleskiw, Yakubovich, & Peyré, 2013; Yakubovich & Elder, 2014) psychophysically. The rationale for their experiment was that if subjects reached their subjective recognition threshold for a specific animal category when represented by a given shape descriptor with fewer components (ranging from 1–10), one might argue that this representation is closer to the encoding scheme employed by the human visual system. Their results show that shapelets had the lowest threshold (i.e. number of components), supporting the idea that the visual system utilizes localized basis functions which tile the whole shape (Fruend & Elder, 2013). Fruend and Elder (2015)'s results are in keeping with the shape coding representation hypothesized by Pasupathy and Connor (2002), who described single cells in primate area V4 tuned to contours with specific features, e.g. convex and concave curvature, relative to the shapes' center or Carlson, Rasquinha, Zhang, and Connor (2011), who suggest that the sparse coding of objects is reflected in the bias of V4 neurons towards less frequent object features, i.e., acute curvature maxima, and a more pronounced representation of uncommon, but salient shape features, which contain most information about object identity. The characteristic, localized basis functions of shapelets are reminiscent of the population code models proposed by Pasupathy and Connor (2002) and
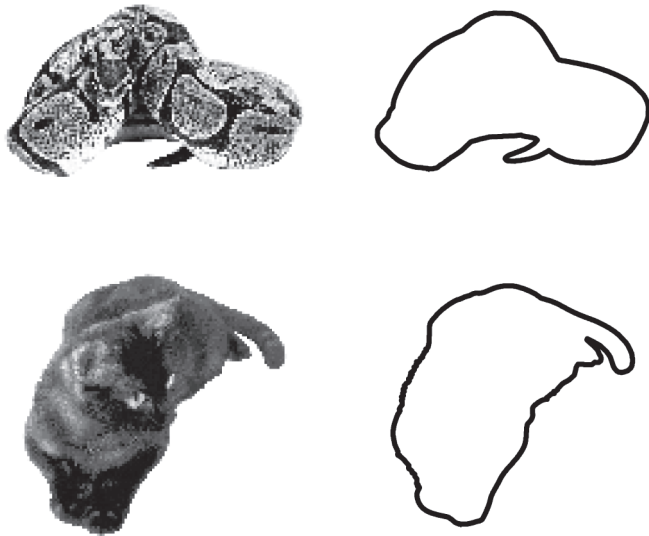
Fig. 8. Shapes from outlines The figure shows two black and white images from the Hemera database (left) and the corresponding extracted boundaries of these images (right).

Carlson et al. (2011).

It is important to mention, however, that the assumptions made here are only applicable to smooth, two-dimensional shapes, defined by their one-dimensional boundary (outline). Shape representation based on such simple shape features is most likely a simplification, because the visual system is consistently confronted with objects which are partly covered or occluded by other objects or by an object's own features. Consider for instance the silhouettes of the animals depicted in Fig. 8. One can clearly see that the boundary information is not sufficient to extract crucial information about the original object because some features, such as the folded body of the snake or the head of the cat, occlude the rest of its body rendering them completely inaccessible. Hence, simply extracting the boundary of an object cannot explain the entirety of shape representation. Instead, mechanisms that process other cues, like shading, perspective, texture gradients etc. are important features too. Further research is necessary to develop shape encoding schemes that take such aspects into account.

In summary, our results suggest that compound RF patterns can represent only a small and perceptually distinct subset of possible planar shapes. Due to their mathematical limitations they are not suited as universal shape descriptors utilized by the visual system. Yet, it may be that (compound) RF patterns describe a behaviourally relevant subset of planar shape outlines. It is important to keep in mind that restricting studies to only RF compounds implicitly restricts them to only certain ranges of perceptually meaningful dimensions and we believe that it is important to be aware of possible overinterpretations when interpreting results obtained with only RF patterns and compounds.

Acknowledgements

References

Alter, I., & Schwartz, E. L. (1988). Psychophysical studies of shape with fourier descriptor stimuli. *Perception, 17*, 191–202.

Bell, J., & Badcock, D. R. (2008). Luminance and contrast cues are integrated in global shape detection with contours. *Vision Research, 48*, 2336–2344.

Bell, J., & Badcock, D. R. (2009). Narrow-band radial frequency shape channels revealed by sub-threshold summation. *Vision Research, 49*, 843–850.

Bell, J., Badcock, D. R., Wilson, H., & Wilkinson, F. (2007). Detection of shape in radial frequency contours: Independence of local and global form information. *Vision Research, 47*, 1518–1522.

Bell, J., Wilkinson, F., Wilson, H. R., Loffler, G., & Badcock, D. R. (2009). Radial frequency adaptation reveals interacting contour shape channels. *Vision Research, 49*, 2306–2317.

Biederman, I. (1987). Recognition-by-components: A theory of human image understanding. *Psychological Review, 94*, 115–147.

Cappé, O., Guilin, A., Marin, J. M., & Robert, C. P. (2004). Population monte carlo. *Journal of Computational and Graphical Statistics, 13*, 907–929.

Carlson, E. T., Rasquinha, R. J., Zhang, K., & Connor, C. E. (2011). A sparse object coding scheme in area v4. *Current Biology, 21*, 288–293.

DiCarlo, J. J., Zoccolan, D., & Rust, N. C. (2012). How does the brain solve visual object recognition? *Neuron, 73*, 415–434.

Dickinson, J. E., Bell, J., & Badcock, D. R. (2013). Near their thresholds for detection, shapes are discriminated by the angular separation of their corners. *PloS one, 8*, e66015 .

Dickinson, J. E., Haley, K., Bowden, V. K., & Badcock, D. R. (2018). Visual search reveals a critical component to shape. *Journal of Vision, 18* 2–2.

Dubinskiy, A., & Zhu, S. C. (2003). A multi-scale generative model for animate shapes and parts. *Computer Vision* (pp. 249–256). IEEE.

Ehinger, K. A., & Wolfe, J. M. (2016). How is visual search guided by shape? using features from deep learning to understand preattentive shape space. *Vision Science Society 16th Annual Meeting.*.

Elder, J., Oleskiw, T., & Fruend, I. (2018). The role of global cues in the perceptual grouping of natural shapes. *Journal of Vision* in revision.

Elder, J. H., Oleskiw, T. D., Yakubovich, A., & Peyré, G. (2013). On growth and formlets: Sparse multi-scale coding of planar shape. *Image and Vision Computing, 31*, 1–13.

Fruend, I., & Elder, J. (2013). Statistical coding of natural closed contours. *Journal of Vision, 13* 119–119, VSS abstract.

Fruend, I., & Elder, J. (2015). Psychophysical evaluation of planar shape representations for object recognition. *Journal of Vision, 15* 522–522, VSS abstract.

Gauthier, I., & Tarr, M. J. (2016). Visual object recognition: Do we (finally) know more now than we did? *Annual Review of Vision Science, 2*, 377–396.

Green, R. J., Dickinson, J. E., & Badcock, D. R. (2017). Global processing of random-phase radial frequency patterns but not modulated lines. *Journal of Vision, 17* 18–18.

Green, R. J., Dickinson, J. E., & Badcock, D. R. (2018a). The effect of spatiotemporal displacement on the integration of shape information. *Journal of Vision, 18* 4–4.

Green, R. J., Dickinson, J. E., & Badcock, D. R. (2018b). Integration of shape information occurs around closed contours but not across them. *Journal of Vision, 18* 6–6.

Hess, R. F., Achtman, R. L., & Wang, Y.-Z. (2001). *Detection of contrast-defined shape. JOSA A, 18*, 2220–2227.

Jeffrey, B. G., Wang, Y.-Z., & Birch, E. E. (2002). Circular contour frequency in shape discrimination. *Vision Research, 42*, 2773–2779.

Kristjánsson, Á., & Tse, P. U. (2001). Curvature discontinuities are cues for rapid shape analysis. *Perception & Psychophysics, 63*, 390–403.

Lawrence, S. J., Keefe, B. D., Vernon, R. J., Wade, A. R., McKeefry, D. J., & Morland, A. B. (2016). Global shape aftereffects in composite radial frequency patterns. *Journal of Vision, 16* 17–17.

Loffler, G. (2008). Perception of contours and shapes: Low and intermediate stage mechanisms. *Vision Research, 48*, 2106–2127.

Loffler, G. (2015). Probing intermediate stages of shape processing. *Journal of Vision, 15*, 1–19.

Loffler, G., Wilson, H. R., & Wilkinson, F. (2003). Local and global contributions to shape discrimination. *Vision Research, 43*, 519–530.

Marr, D., & Nishihara, H. K. (1978). Representation and recognition of the spatial organization of three-dimensional shapes. *Proceedings of the Royal Society of London, Series B: Biological Sciences, 200*, 269–294.

Mayya, N., & Rajan, V. T. (1996). Voronoi diagrams of polygons: A framework for shape representation. *Journal of Mathematical Imaging and Vision, 6*, 355–378.

Pasupathy, A., & Connor, C. E. (2002). Population coding of shape in area v4. *Nature Neuroscience, 5*, 1332.

Peirce, J. W. (2007). Psychopy–psychophysics software in python. *Journal of Neuroscience Methods, 162*, 8–13.

Pinto, N., Cox, D. D., & DiCarlo, J. J. (2008). Why is real-world visual object recognition hard? *PLoS Computational Biology, 4*, e27 .

Poirier, F. J., & Wilson, H. R. (2006). A biologically plausible model of human radial frequency perception. *Vision Research, 46*, 2443–2455.

Ramsey, P. H. (1989). Critical values for spearman's rank order correlation. *Journal of Educational Statistics, 14*, 245–253.

Salmela, V. R., Henriksson, L., & Vanni, S. (2016). Radial frequency analysis of contour shapes in the visual cortex. *PLoS Computational Biology, 12*, e1004719 .

Schmidtmann, G., Jennings, B. J., & Kingdom, F. A. (2015). Shape recognition: convexities, concavities and things in between. *Scientific Reports, 5*, 17142.

Schmidtmann, G., Kennedy, G. J., Orbach, H. S., & Loffler, G. (2012). Non-linear global pooling in the discrimination of circular and non-circular shapes. *Vision Research, 62*, 44–56.

Thorpe, S., Fize, D., & Marlot, C. (1996). Speed of processing in the human visual system. *Nature, 381*, 520–522.

Treisman, A., & Souther, J. (1985). Search asymmetry: A diagnostic for preattentive processing of separable features. *Journal of Experimental Psychology: General, 114*, 285.

Watson, A. B., & Pelli, D. G. (1983). Quest: A bayesian adaptive psychometric method. *Perception & Psychophysics, 33*, 113–120.

Wilkinson, F., James, T. W., Wilson, H. R., Gati, J. S., Menon, R. S., & Goodale, M. A.

(2000). An fmri study of the selective activation of human extrastriate form vision areas by radial and concentric gratings. *Current Biology, 10*, 1455–1458.

Wilkinson, F., Wilson, H. R., & Habak, C. (1998). Detection and recognition of radial frequency patterns. *Vision Research, 38*, 3555–3568.

Wilson, H. R., Loffler, G., & Wilkinson, F. (2002). Synthetic faces, face cubes, and the geometry of face space. *Vision Research, 42*, 2909–2923.

Wilson, H. R., & Wilkinson, F. (2002). Symmetry perception: A novel approach for biological shapes. *Vision Research, 42*, 589–597.

Wilson, H. R., Wilkinson, F., Lin, L.-M., & Castillo, M. (2000). Perception of head orientation. *Vision Research, 40*, 459–472.

Wolfe, J. M., & Horowitz, T. S. (2004). What attributes guide the deployment of visual attention and how do they do it? *Nature Reviews Neuroscience, 5*, 495.

Wolfe, J. M., & Horowitz, T. S. (2017). Five factors that guide attention in visual search. *Nature Human Behaviour, 1*, 0058.

Yakubovich, A., & Elder, J. H. (2014). Building better formlet codes for planar shape. IEEE.

Zahn, C. T., & Roskies, R. Z. (1972). Fourier descriptors for plane closed curves. *IEEE Transactions on computers, 100*, 269–281.